Journal of Natural History

ISSN: (Print) (Online) Journal homepage: https://www.tandfonline.com/loi/tnah20

Adding missing vines to the tree: multilocus phylogeny of New World vine snakes (Serpentes: Colubridae: *Oxybelis*), with description of a new species

Omar Torres-Carvajal, Mauricio Mejía-Guerrero & Claudia Terán

To cite this article: Omar Torres-Carvajal, Mauricio Mejía-Guerrero & Claudia Terán (2021) Adding missing vines to the tree: multilocus phylogeny of New World vine snakes (Serpentes: Colubridae: *Oxybelis*), with description of a new species, Journal of Natural History, 55:31-32, 2027-2046, DOI: 10.1080/00222933.2021.1986164

To link to this article: https://doi.org/10.1080/00222933.2021.1986164

JOURNAL OF NATURAL HISTORY
2021, VOL. 55, NOS. 31–32, 2027–2046
https://doi.org/10.1080/00222933.2021.1986164

Adding missing vines to the tree: multilocus phylogeny of New World vine snakes (Serpentes: Colubridae: *Oxybelis*), with description of a new species

Omar Torres-Carvajal, Mauricio Mejía-Guerrero and Claudia Terán

Museo de Zoología, Departamento de Ciencias Biológicas, Pontificia Universidad Católica del Ecuador, Quito, Ecuador

ABSTRACT

Neotropical vine snakes (*Oxybelis*) have a wide distribution range from southern United States to southeastern Brazil. Notably, the widespread brown vine snake *O. aeneus* was recently split into eight species, but major geographical areas such as the South American Pacific lowlands remained unsampled. In this paper, we present the largest molecular phylogeny of *Oxybelis* to date using six mitochondrial and nuclear genes and 10 of the 11 currently recognised species of *Oxybelis*. Our analyses include the first South American samples from west of the Andes, which we describe as a new species based on molecular and morphological evidence. The new species is morphologically most similar to *O. acuminatus, O. aeneus*, and *O. inkaterra*. Although the new species is genetically distinctive and divergent from its congeners, its phylogenetic placement received low support. Our results also suggest that a sample from Escudo de Veraguas Island in Panama represents an undescribed species of *Oxybelis*. Finally, we clarify the phylogenetic position of *O. aeneus* sensu stricto.

https:urn:lsid:zoobank.org:pub:CC4E3741-D9DF-4F6C-8D0F-9BD20CB124E5

ARTICLE HISTORY
Received 21 May 2021
Accepted 21 September 2021

KEYWORDS
Biodiversity; phylogenetics; Serpentes; South America; taxonomy

Introduction

The Neotropics represent the largest species richness hotspot of snakes worldwide (Roll et al. 2017). Strikingly, recent systematic studies suggest that snake diversity in the Neotropics is probably much higher as multiple evolutionary lineages are often mistaken for single, widely distributed species (Melo-Sampaio et al. 2021). One of the most widespread snake taxa of the Americas is *Oxybelis* Wagler, a clade of vine snakes traditionally ranked as a genus. Until recently, only four species of *Oxybelis* were recognised – *O. aeneus* Wagler 1824, *O. brevirostris* Cope 1861, *O. fulgidus* Daudin 1803, and *O. wilsoni* Villa and McCranie 1995. Notably, the brown vine snake *O. aeneus* sensu lato is the most widespread species occurring from southern United States to northern Peru (west of the Andes), Bolivia (east of the Andes), and southeastern Brazil (Keiser 1974, 1982).

CONTACT Omar Torres-Carvajal omartorcar@gmail.com
Supplemental data for this article can be accessed here.

Published online 03 Nov 2021

Although several species or subspecies within *O. aeneus* sensu lato had been proposed, Keiser (1974) concluded that there was no evidence to split *O. aeneus* sensu lato into different taxa based on a comprehensive morphological study of over 1,200 specimens from throughout its range. More recently, based on multivariate morphological analyses, phylogenetic analyses of mitochondrial and nuclear DNA, as well as species delimitation analyses under a multispecies coalescent Jadin et al. (2019, 2020, 2021) split *O. aeneus* sensu lato into eight species including four resurrected synonyms – *O. acuminatus* Wied 1824, *O. aeneus, O. inkaterra* Jadin et al. 2021, *O. koehleri* Jadin et al. 2020, *O. microphthalmus* Barbour and Amaral 1926, *O. potosiensis* Taylor 1941, *O. rutherfordi* Jadin et al. 2020, and *O. vittatus* Girard 1854. Remarkably, these authors recognised important geographic barriers, such as the Isthmus of Tehuantepec, Isthmus of Panama, and Andes Mountains separating species within the *O. aeneus* complex and restricted the distribution of *O. aeneus* sensu stricto to the Amazon Basin. Jadin et al. (2019, 2020, 2021) did not explicitly include *O. aeneus* sensu stricto in their phylogenetic analyses and they did not examine any specimens of *O. aeneus* sensu lato from northern South America west of the Andes (i.e. Pacific coast of Colombia, Ecuador and Peru).

In this paper, we present a molecular phylogeny of *Oxybelis* that includes all currently known species except *O. acuminatus*. We also use morphological and molecular evidence to describe a new species of the *O. aeneus* complex from the Pacific lowlands in western Ecuador. Finally, we clarify the phylogenetic position of *O. aeneus* sensu stricto.

Material and methods

Laboratory protocols and sampling

We generated novel DNA sequences from 10 specimens from Ecuador representing *Oxybelis brevirostris* (N = 2), *O. fulgidus* (N = 2), *O. inkaterra* (N = 1) and a new species of the *O. aeneus* complex described below (N = 5). In addition, we obtained sequences of 60 specimens from GenBank representing nine of the 11 recognised species of *Oxybelis*, as well as *Leptophis depressirostris* and *Chironius exoletus*, which were used as outgroups (Jadin et al. 2019). We excluded from our analyses four 16S sequences of *Oxybelis vittatus* (USNMFS195259, 195260, 195366, 195398) from Escudo de Veraguas Island and nine of *O. brevirostris* (BSFS8810, BSFS8822, JM351, JM435, JM488, JM721, JM752, JM804, JM805) from Torrijos National Park in Panama (D. Mulcahy unpubl. data) because they were identical to other sequences of conspecifics from the same localities (USNM347529 and BSFS4610, respectively). Specimens included in our analyses are listed in Table 1.

We isolated DNA from frozen muscle or liver tissues using a guanidine isothycianate protocol (Torres-Carvajal and Hinojosa 2020). We obtained nucleotide sequences from four mitochondrial genes, ribosomal small (12S, 373 aligned sites) and large (16S, 493) subunit genes, cytochrome b (CYTB, 1077), subunit IV of NADH dehydrogenase (ND4, 666), as well as two nuclear genes, oocyte maturation factor MOS (CMOS, 558) and prolactin receptor (PRLR, 477). Polymerase Chain Reaction (PCR) amplification of gene fragments was performed in a final volume of 25 µl reactions using 1X PCR Buffer (–Mg), 3 mM $MgCl_2$, 0.2 mM dNTP mix, 0.2 µM of each primer, 0.1 U/µl of Platinum® Taq DNA

Table 1. Vouchers, locality data, and GenBank accession numbers of taxa and gene regions analysed in this study. Newly sequenced specimens are marked with an asterisk.

Taxon	Voucher and locality	GenBank accession number					
		CYTB	ND4	12S	16S	CMOS	PRLR
Chironius exoletus	QCAZ 13303. ECUADOR: Morona Santiago: Puyo-Macas road.	OK143277*	MK086856	MK086656	MK086553	MK086755	–
Leptophis depressirostris	FN253772. Unknown locality.	KR814686	KR814724	KR814617	KR814643	KR814682	–
Oxybelis aeneus	R6911. BRAZIL: Tocantins: Luiz Eduardo Magalhães Hydroelectric Powerplant.	–	–	HM565765	HM582225	HQ157829	–
Oxybelis brevirostris	BSFS 4610. PANAMA. Cocle: El Cope.	–	–	–	MH140885	–	–
Oxybelis brevirostris	BSFS 4594. PANAMA. Cocle: El Cope.	–	–	–	MH140893	–	–
Oxybelis brevirostris	JMR 2013-020. PANAMA.	MT969178	MT969199	MT969241	MT969275	MT969311	–
Oxybelis brevirostris	UTA R-55952. ECUADOR: Esmeraldas: San Lorenzo.	MT969179	–	–	–	MT969312	–
Oxybelis brevirostris	LSUMZ H-12770. ECUADOR: Imbabura.	MT969180	MT969200	MT969242	MT969276	MT969313	–
Oxybelis brevirostris	QCAZ 16498. ECUADOR: Guayas: Centro Shuar Tsuer Entsa. Lat. −2.78, Long. −79.64	OK143278*	OK149138*	OK129312*	OK129302*	OK149147*	OK149160*
Oxybelis brevirostris	QCAZ 16946. ECUADOR: Manabí: Manglares-Churute Ecological Reserve. Lat. 0.34, Long. −79.72	OK143279*	OK149139*	OK129313*	OK129303*	OK149148*	OK149161*
Oxybelis fulgidus	MBLUZ 1480. VENEZUELA: Bolivar.	MT969183	MT969210	MT969250	MT969286	–	
Oxybelis fulgidus	MZUSP11417. BRAZIL: Mato Grosso	MK209278	–	MK209203	MK209316	–	–
Oxybelis fulgidus	No voucher. FRENCH GUIANA: Saint Eugène, Petit Saut.	–	–	AF158432	AF158497	–	–
Oxybelis fulgidus	No voucher. SURINAME.	MH122703	–	–	–	–	–
Oxybelis fulgidus	No voucher. Locality unknown.	–	–	–	HM582226	HQ157830	–
Oxybelis fulgidus	QCAZ 5206. ECUADOR: Orellana: Vía Pompeya Sur – Iro, km 74. Lat. −0.84, Long. −76.35	OK143280*	–	OK129314*	OK129304*	OK149149*	OK149162*
Oxybelis fulgidus	QCAZ 14078. ECUADOR: Pastaza: Comunidad Paparahua, Campo Villano. Lat. −1.48, Long. −77.41	OK143281*	OK149140*	OK129315*	OK129305*	OK149150*	OK149163*
Oxybelis fulgidus	UTA R-52506. MEXICO: Veracruz.	MK497173	MT969201	MT969243	MT969277	MK497197	MK497219
Oxybelis fulgidus	UTA R-53002. MEXICO: Oaxaca.	MK497174	MT969202	MT969244	MT969278	MK497198	MK497220
Oxybelis fulgidus	JAC 24318. MEXICO: Chiapas.	MK497175	MT969203	MT969245	MT969279	MK497199	MK497221
Oxybelis fulgidus	UTA R-53417. MEXICO: Yucatan.	MK497176	MT969204	–	MT969280	MK497200	MK497222
Oxybelis fulgidus	UTA R-45292. GUATEMALA: Izabal.	MK497177	MT969205	–	MT969281	MK497201	MK497223
Oxybelis fulgidus	MSM 439. HONDURAS: Comayagua.	MK497178	MT969206	MT969246	MT969282	MK497202	–
Oxybelis fulgidus	USNM 565820. HONDURAS: Olancho.	MK497179	MT969207	MT969247	MT969283	MK497203	MK497224
Oxybelis fulgidus	LSUMZ H-6358. HONDURAS.	MT969181	MT969208	MT969248	MT969284	MT969314	–
Oxybelis fulgidus	LSUMZ H-6352. Unknown locality.	MT969182	MT969209	MT969249	MT969285	MT969315	–
Oxybelis inkaterra	QCAZ 5207. ECUADOR: Orellana: Parque Nacional Yasuní. Lat. −0.63, Long. −76.46	OK143282*	OK149141*	OK129316*	OK129306*	OK149151*	OK149157*
Oxybelis koehleri	UTA R-46846. GUATEMALA: Zacapa.	MK497189	MT969211	MT969251	MT969287	MK497212	–
Oxybelis koehleri	UTA R-46865. HONDURAS: Comayagua.	MK497190	MT969212	MT969252	MT969288	MK497213	MK497232
Oxybelis koehleri	UTA R-44838. NICARAGUA: Jinotega.	MK497191	MT969213	MT969253	MT969289	MT969316	MK497233

(*Continued*)

Table 1. (Continued).

Taxon	Voucher and locality	GenBank accession number					
		CYTB	ND4	12S	16S	CMOS	PRLR
Oxybelis koehleri	KU R-288907. EL SALVADOR.	MT969184	MT969214	MT969254	MT969290	MT969317	–
Oxybelis koehleri	LSUMZ H-6353. Unknown locality.	MT969185	MT969215	MT969255	MT969291	MT969318	–
Oxybelis microphthalmus	JAC 30618. MEXICO: Sinaloa.	MT969186	MT969216	MT969256	–	MK497204	MK497225
Oxybelis microphthalmus	UTA R-53331. MEXICO: Nayarit.	MK497180	MT969217	–	MT969292	MK497205	MK497226
Oxybelis microphthalmus	UTA R-53373. MEXICO: Jalisco.	MK497181	MT969218	–	MT969293	MK497206	MK497227
Oxybelis microphthalmus	UTA R-57658. MEXICO: Colima.	MK497182	MT969219	–	–	–	–
Oxybelis microphthalmus	UTA R-57659. MEXICO: Colima.	MK497183	MT969220	–	MT969294	MK497207	–
Oxybelis microphthalmus	UTA R-53374. MEXICO: Jalisco.	MK497184	MT969221	–	–	MK497208	MK497228
Oxybelis microphthalmus	MZFC 19224. MEXICO: Guerrero.	MK497185	MT969222	MT969257	MT969295	MK497209	MK497229
Oxybelis microphthalmus	UTA R-53024. MEXICO: Guerrero.	MK497186	MT969223	MT969258	MT969296	MK497210	MK497230
Oxybelis microphthalmus	UTA R-53026. MEXICO: Oaxaca.	MK497187	MT969224	MT969259	MT969297	–	
Oxybelis microphthalmus	UTA R-52648 MEXICO: Oaxaca.	MK497188	MT969225	MT969260	MT969298	MK497211	MK497231
Oxybelis microphthalmus	UTA R-53021. MEXICO: Michoacan.	MT969187	MT969226	MT969261	MT969299	MT969319	–
Oxybelis microphthalmus	UTA R-53427. MEXICO: Oaxaca.	MT969188	MT969227	MT969262	–	MT969320	–
Oxybelis microphthalmus	CAS 175557. USA: Arizona, Santa Cruz Co.	AF471056	–	–	–	AF471148	–
Oxybelis potosiensis	MZFC 17581. MEXICO: Yucatan.	MT969189	MT969228	MT969263	MT969300	MT969321	–
Oxybelis potosiensis	UTA R-52600. MEXICO: Puebla.	MT969190	MT969229	MT969264	MT969301	MT969322	MT969330
Oxybelis rutherfordi	MNHN 1996.7855. FRENCH GUIANA: Petit Saut.	–	–	AF158416	AF158498	–	–
Oxybelis rutherfordi	UWIZM.2011.18.10. TOBAGO.	MK497193	MT969230	–	–	MK497215	–
Oxybelis rutherfordi	UWIZM.2012.27.49. TOBAGO.	MK497194	–	–	–	MK497216	–
Oxybelis rutherfordi	UWIZM.2011.20.14. TRINIDAD.	MK497195	MT969231	MT969265	MT969302	MK497217	MT969331
Oxybelis rutherfordi	UWIZM.2016.23.5. TRINIDAD.	MK497196	–	–	–	MK497218	–
Oxybelis rutherfordi	LSUMZ H-6608. VENEZUELA: Sucre.	MT969191	MT969232	MT969266	MT969303	MT969323	–

(*Continued*)

Table 1. (Continued).

Taxon	Voucher and locality	GenBank accession number					
		CYTB	ND4	12S	16S	CMOS	PRLR
Oxybelis rutherfordi	MBLUZ 1268. VENEZUELA: Isla Margarita.	MT969192	MT969233	MT969267	MT969304	–	–
Oxybelis transandinus	QCAZ 4463. ECUADOR: Loja: Puyango Petrified Forest. Lat. −3.89, Long. −80.07	OK143283*	OK149142*	OK129317*	OK129307*	OK149152*	OK149164*
Oxybelis transandinus	QCAZ 15804. ECUADOR: Azuay: Sulupali. Lat. −3.35, Long. −79.31	OK143286*	OK149145*	OK129320*	OK129310*	OK149155*	OK149158*
Oxybelis transandinus	QCAZ 16331. ECUADOR: Guayas: Manglares-Churute Ecological Reserve. Lat. −2.4, Long. −79.65	OK143287*	OK149146*	OK129321*	OK129311*	OK149156*	OK149159*
Oxybelis transandinus	QCAZ 17096. ECUADOR: Azuay: San Juan. Lat. −2.23, Long. −79.14	OK143284*	OK149143*	OK129318*	OK129308*	OK149153*	OK149165*
Oxybelis transandinus	QCAZ 17097 (holotype). ECUADOR: Guayas: Bosqueira Protected Forest. Lat. −2.01, Long. −79.98	OK143285*	OK149144*	OK129319*	OK129309*	OK149154*	OK149166*
Oxybelis vittatus	ENS 11259. PANAMA: Coiba Island.	MK497192	MT969234	MT969268	MT969305	MK497214	MK497234
Oxybelis vittatus	JMR 2013-016. PANAMA.	MT969193	MT969235	MT969269	MT969306	MT969324	–
Oxybelis vittatus	JMR 2013-019. PANAMA.	MT969194	MT969236	MT969270	MT969307	MT969325	–
Oxybelis vittatus	JMR UNK020. PANAMA.	MT969195	MT969237	MT969271	–	MT969326	–
Oxybelis vittatus	JMR 2013-025. PANAMA.	MT969196	MT969238	MT969272	MT969308	MT969327	–
Oxybelis vittatus	JMR 2013-105. PANAMA.	MT969197	MT969239	MT969273	MT969309	MT969328	–
Oxybelis vittatus	JMR UNK015. PANAMA.	MT969198	MT969240	MT969274	MT969310	MT969329	–
Oxybelis vittatus	CH 6080. PANAMA: Balboa, San Miguel, Isla de Canas, Playa Lagarto.	–	–	–	MH140879	–	–
Oxybelis vittatus	CH 5078. PANAMA: Cocle, Cascajal river, Cascajal.	–	–	–	MH140884	–	–
Oxybelis wilsoni	FN253879. HONDURAS: Roatán Island.	KR814689	KR814710	KR814626	KR814647	KR814669	–
Oxybelis sp.	USNM 347529. PANAMA: Bocas del Toro: Escudo de Veraguas Island, west point.	–	–	–	MH140878	–	–

Polymerase (Invitrogen, Carlsbad, CA) and 1 µl of extracted DNA. PCR primers, protocols, and amplicon lengths are presented in Table 2. Double stranded sequencing of the PCR products was performed in both directions by Macrogen Inc. (Seoul, Korea).

Except for QCAZ specimens from Ecuador, we did not examine any of the voucher specimens corresponding to the sequences used in phylogenetic analyses. GenBank sequences of '*O. aeneus*' not included in previous publications were assigned to corresponding species based on phylogenetic relationships. Our final dataset had 70 terminals representing two outgroup species, 10 of the 11 currently recognised species of *Oxybelis*, and two undescribed species of *Oxybelis* (Table 1).

Phylogenetic analyses

Data were assembled and aligned in Geneious v9.1.8 (Kearse et al. 2012) under default settings for MAFFT (Algorithm: Auto, Scoring Matrix: 200PAM/k = 2, Gap open penalty: 1.53, Offset value: 0.123; Katoh and Standley 2013). Ribosomal (12S and 16S) gene regions with multiple gaps were realigned to minimise indels and optimise nucleotide identities among different individuals. Sequences of CYTB, ND4, CMOS and PRLR were translated into amino acids for confirmation of alignment. After partitioning the concatenated dataset (Data S1) by gene (12S, 16S) and codon position (CYTB, ND4, CMOS, PRLR), we chose the best-fit nucleotide substitution models and partitioning scheme simultaneously

Table 2. Gene regions, primers, PCR protocols and PCR products used in this study. F = forward, R = reverse.

Gene region	Primer Sequence (5′–3′)	PCR protocol	Mean amplicon length (nucleotides)	Aligned nucleotides
CYTB	**F: L14910** (Burbrink et al. 2000) GACCTGTGATMTGAAAACCAY **R: H16064** (Burbrink et al. 2000) CTTTGGTTTACAAGAACAATGCTTTA	1 cycle: 2 min 94°C 40 cycles: 30 s 94°C, 30 s 48°C, 1 min 72°C 1 cycle: 10 min 72°C	1122.9	1077
ND4	**F: ND4** (Arévalo, Davis, & Sites Jr., 1994) CACCTATGACTACCAAAAGCTCATGT **R: ND413824H** (Arévalo et al. 1994) CATTACTTTTACTTGGATTTGCACCA	1 cycle: 3.5 min 94°C, 1 min 42°C, 1.5 min 68°C 40 cycles: 30 s 94°C, 30 s 52°C, 1 min 72°C 1 cycle: 15 min 72°C	907.3	666
12S	**F: L1091** (Kocher et al. 1989) CAAACTAGGATTAGATACCCTACTAT **R: H1557** (Knight and Mindell 1994) GTACACTTACCTTGTTACGAC	1 cycle: 3 min 94°C 45 cycles: 30 s 94°C, 30 s 55°C, 1 min 72°C 1 cycle: 10 min 72°C	486.3	373
16S	**F: L2510** (Palumbi et al. 1992) CCGACTGTTTAMCAAAAACA **R: H3056** (Palumbi et al. 1992) CTCCGGTCTGAACTCAGATCACGTAGG	1 cycle: 3 min 96°C 40 cycles: 30 s 95°C, 1 min 51°C, 1 min 72°C 1 cycle: 10 min 72°C	532.9	493
CMOS	**F: S77** (Lawson et al. 2005) CATGGACTGGGATCAGTTATG **R: S78** (Lawson et al. 2005) CCTTGGGTGTGATTTTCTCACCT	1 cycle: 2 min 94°C 40 cycles: 30 s 94°C, 30 s 55°C, 1 min 72°C 1 cycle: 10 min 72°C	588.4	558
PRLR	**F: PRLR-F1** (Townsend et al. 2008) GACARYGARGACCAGCAACTRATGCC **R: PRLR-R3** (Townsend et al. 2008) GACYTTGTGRACTTCYACRTAATCCA	1 cycle: 2 min 94°C 40 cycles: 30 s 94°C, 30 s 50°C, 1 min 72°C 1 cycle: 10 min 72°C	578.3	477

using PartitionFinder v2 (Guindon et al. 2010; Lanfear et al. 2017) under both the Bayesian Information Criterion (BIC) and the 'greedy' algorithm (Lanfear et al. 2012) with branch lengths of alternative partitions 'linked' to search for the best-fit scheme.

We used the CIPRES Science Gateway (Miller et al. 2010) for phylogenetic analyses of the partitioned dataset with the programs MrBayes v3.2.1 (Ronquist et al. 2012) and RAxML v8.2.10 (Stamatakis 2014). The Bayesian analysis consisted of four independent runs, each with four MCMC chains, set for 10 million generations sampling every 1,000 generations. Results were analysed in Tracer v1.7 (Rambaut 2018) to assess convergence and effective sample sizes (≥200) for all parameters. Additionally, we verified that the potential scale reduction factor of all the estimated parameters approached values of 1. Of the 10,000 trees resulting per run, 1,000 were discarded as 'burn-in'. We combined the resultant 36,000 trees in LogCombiner (Rambaut and Drummond 2019a) and used them to calculate posterior probabilities (PP) for each bipartition on a Maximum Clade Credibility Tree in TreeAnnotator (Rambaut and Drummond 2019b). The ML analysis was performed under the GTRGAMMA model. Nodal support (BS) was assessed with the rapid bootstrapping algorithm (Alexandros Stamatakis et al. 2008) and 1,000 replicates. Phylogenetic trees were visualised and edited using FigTree v1.4.2 (Rambaut 2018). Additionally, uncorrected genetic distances among species of *Oxybelis* were calculated in DIVEIN (Deng et al. 2010) for all mitochondrial genes.

Measurements and lepidosis

Specimens (N = 18) of the new species described here are deposited at Museo de Zoología, Pontificia Universidad Católica del Ecuador, Quito (QCAZ). They were collected during several field trips to different localities in western Ecuador between 1987 and 2018. We recorded snout-vent length (SVL) and tail length (TL) with a ruler to the nearest 0.1 cm. Lepidosis terminology follows previous work (Keiser 1974; Jadin et al. 2020), whereas the method of ventral counting follows Dowling (1951). Species comparisons were based on descriptions by Jadin et al. (2020, 2021).

Results

Phylogeny

Selected partitions and models (in brackets) were (1) PRLR-2nd and 3rd codon positions, ND4-1st codon position, CYTB-1st codon position, 12S, 16S [GTR+I+G]; (2) ND4-2nd codon position, CYTB-2nd codon position, CMOS-3rd codon position [HKY+I]; (3) ND4-3rd codon position, CYTB-3rd codon position [GTR+G]; and (4) PRLR-1st codon position, CMOS-1st and 2nd codon positions [K80+I]. The maximum likelihood (ML) and maximum clade credibility (MCC) trees were very similar in topology (Figure 1), with differences only in the position of the trans-Andean samples, as well as in poorly supported terminal nodes. Similar to the recent phylogenetic hypothesis by Jadin et al. (2020), there was strong support for a basal split between the green vine snakes clade (*Oxybelis fulgidus* sensu lato and *O. wilsoni*) and a clade containing all other species of *Oxybelis*. The latter clade is

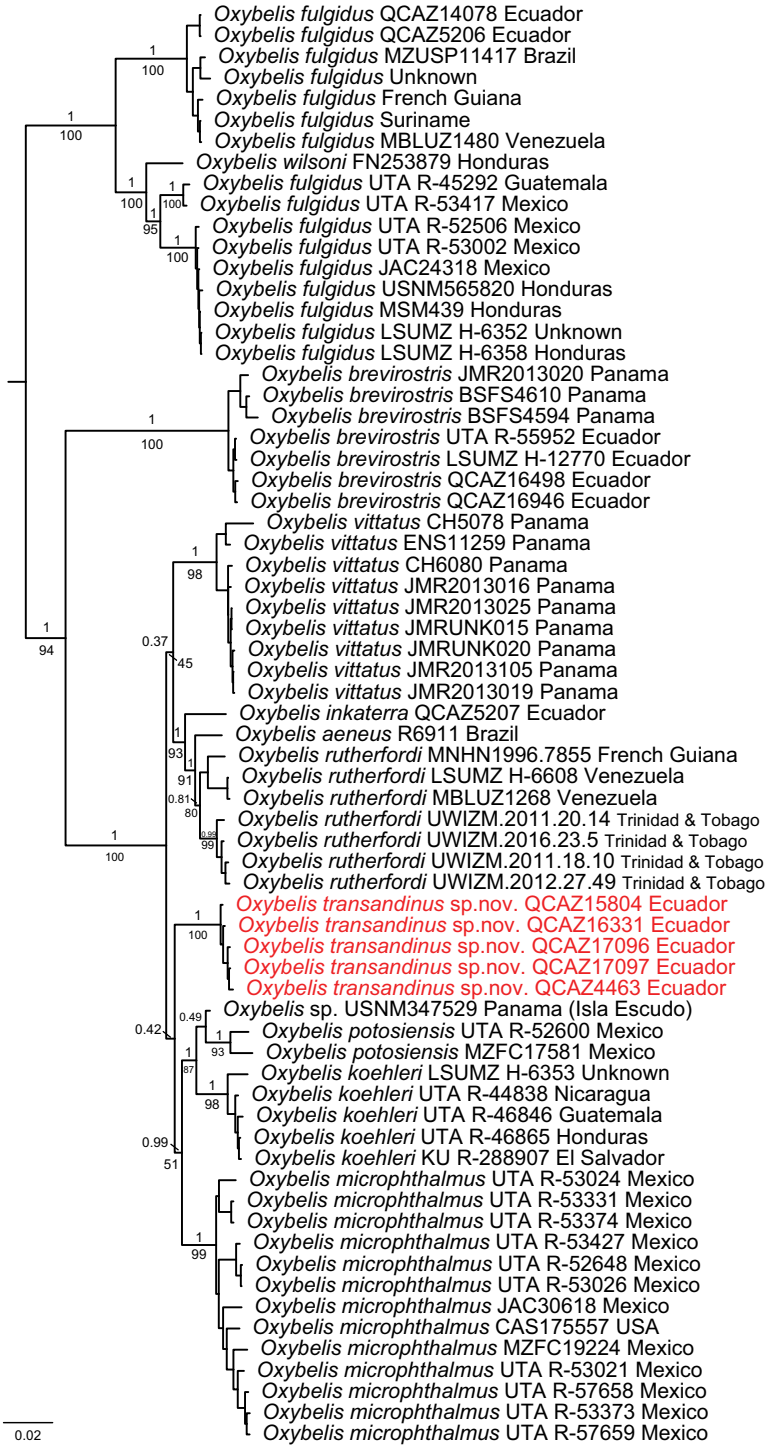

Figure 1. Phylogeny of *Oxybelis*. Maximum clade credibility tree obtained from a phylogenetic analysis of four mitochondrial (12S, 16S, CYTB, ND4) and two nuclear genes (CMOS, PRLR). Posterior probabilities and RAxML rapid-bootstrap support values are shown above and below branches, respectively; for clarity, support values on short branches are not shown. Voucher number and country is

indicated for each terminal. Specimens of the new species described in this paper are coloured in red. Outgroup taxa are not shown. GenBank accession numbers along with more detailed locality data are presented in Table 1.

composed of *O. brevirostris* as sister to the brown vine snakes clade (i.e. *O. aeneus* complex). All species with two or more terminals were recovered as monophyletic with moderate (*O. rutherfordi*) to strong (other species) support, except for *O. fulgidus*. Samples of *O. fulgidus* from Central America were nested in a clade sister to *O. wilsoni*, a species restricted to Isla de Roatán, Honduras. In agreement with previous hypotheses (Jadin et al. 2020), samples of *O. fulgidus* from South America were nested in a different clade sister to (*O. wilsoni, O. fulgidus* Central America). The newly sequenced trans-Andean samples of the *O. aeneus* complex were nested in a maximally supported clade. Within the *O. aeneus* complex (BS = 100, PP = 1), there is a basal split into two poorly supported clades. These clades are similar between the ML and MCC trees, except for the weakly supported position of the trans-Andean clade. In the ML tree, this clade is sister to a larger clade, in which the Panamanian *O. vittatus* is sister to a strongly supported clade (BS = 93, PP = 1) containing, in splitting sequence, *O. inkaterra, O. aeneus* sensu stricto, and *O. rutherfordi*. In the MCC tree, the trans-Andean clade is sister to a larger Northern-Central American clade

Figure 2. Male holotype (QCAZ 17097, total length = 106.3 cm) of *Oxybelis transandinus* **sp. nov**. in life. General views of body (A, B), and dorsal, ventral and lateral views of head (C). Photographs by M. Rivera. Scale bar (C) = 10 mm.

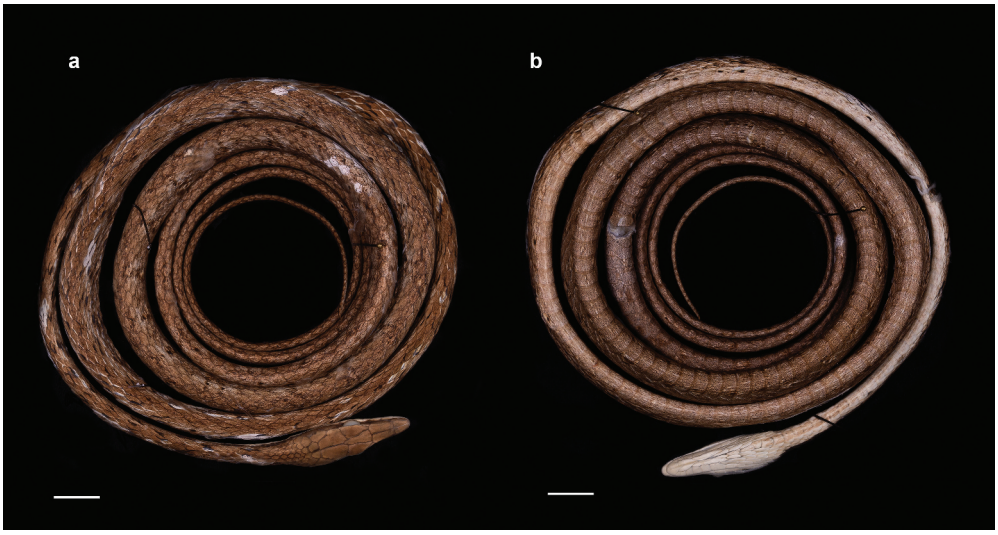

Figure 3. Male holotype (QCAZ 17097, total length = 106.3 cm) of *Oxybelis transandinus* **sp. nov**. in dorsal (A) and ventral (B) views. Photographs by M. Mejía-Guerrero. Scale bars = 10 mm.

(BS = 51, PP = 0.99), in which *O. microphthalmus* is sister to a strongly supported subclade (BS = 87, PP = 1) composed of *O. koehleri, O. potosiensis*, and a sample of an undetermined species (*Oxybelis* sp.) from Escudo de Veragua Island in Panama.

Genetic distances

Interspecific genetic distances are presented in Tables S1–S4. Mean genetic distances range from 0.011 (*O. inkaterra* vs. *O. aeneus*, trans-Andean clade vs. both *O. inkaterra* and *O. aeneus*) to 0.07 (*O. koehleri* vs. *O. wilsoni*) for 12S (mean = 0.039 ± 0.019), 0.003 (*O. koehleri* vs. *O.* sp.) to 0.060 (*O. fulgidus* from South America [SA] vs. *O. aeneus*) for 16S (mean = 0.032 ± 0.014), 0.05 (*O. inkaterra* vs. *O. rutherfordi*) to 0.176 (*O. fulgidus* SA vs. *O. brevirostris*) for CYTB (mean = 0.115 ± 0.044), and 0.040 (*O. fulgidus* from Central America [CA] vs. *O. wilsoni, O. inkaterra* vs. *O. rutherfordi*) to 0.201 (*O. fulgidus* CA vs. trans-Andean clade) for ND4 (mean = 0.121 ± 0.06). Genetic distances among species of the *Oxybelis aeneus* complex range between from 0.011 (*O. inkaterra* vs. *O. aeneus*, trans-Andean clade vs. both *O. inkaterra* and *O. aeneus*)–0.033 (*O. vittatus* vs. both *O. rutherfordi* and *O. potosiensis*) for 12S (mean = 0.020 ± 0.007), 0.003 (*O. koehleri* vs. *O.* sp.2) – 0.032 (*O. rutherfordi* vs. *O. potosiensis*) for 16S (mean = 0.020 ± 0.007), 0.05 (*O. inkaterra* vs. *O. rutherfordi*)–0.076 (trans-Andean clade vs. both *O. inkaterra* and *O. koehleri*) for CYTB (mean = 0.065 ± 0.007), and 0.04 (*O. inkaterra* vs. *O. rutherfordi*)–0.067 (trans-Andean clade vs. *O. potosiensis*) for ND4 (mean = 0.053 ± 0.007).

Systematics

Oxybelis transandinus **sp. nov.**

urn:lsid:zoobank.org:act:80930885-671F-42CE-BF19-1BB1CDA0BD4F

Oxybelis aeneus – Peters (1960), partim; Keiser (1974), partim.

Holotype: QCAZ 17097 (Figures 2, 3), an adult male from Bosqueira Protected Forest (−2.009 latitude, −79.979 longitude, 57 m above sea level; hereafter asl), Guayas Province, Ecuador, collected on 3 October 2018 by A. Achig.

Paratypes (N = 17): ECUADOR: Azuay: QCAZ 15804, adult female from Sulupali, Santa Isabel (−3.347, −79.314, 1,044 m asl), collected on 13 June 2017 by D. Almeida. Cañar: QCAZ 17095-96, adult females from San Juan (−2.226, −79.135, 360 m asl), collected on 27 September 2018 by A. Achig. El Oro: QCAZ 14448, adult male from Arenillas Military Ecological Reserve (−3.503, −80.127, 12 m asl), collected on 11 June 2016 by F. Ayala; QCAZ 17094, adult female from Arenillas Military Ecological Reserve (−3.253, −79.879, 5 m asl), collected on 24 September 2018 by A. Achig. Esmeraldas: QCAZ 583, adult male from Same (0.842, −79.921, 7 m asl) collected on 10 January 1987 by G. Morillo. Guayas: QCAZ 8731, adult female from Cerro Blanco Forest (−2.180, −80.019, 237 m asl) collected on 7 August 2008 by G. Pazmiño; QCAZ 9122, adult female from Cerro Blanco Forest (−2.178, −80.021, 281 m asl) collected on 16 May 2008 by G. Pazmiño; QCAZ 3947, adult female from the banks of Daule river (−2.144, −79.869, 5 m asl), collected on 1 January 1998 by V. Benavides; QCAZ 16331, adult female from Manglares-Churute Ecological Reserve (−2.401, −79.653, 495 m asl) collected on 21 February 2018 by D. Almeida; QCAZ 16039, juvenile from Parque Lago National Recreation Area (−2.215, −80.104, 53 m asl), collected on 29 March 2017 by D. Almeida. Loja: QCAZ 4463, juvenile from Puyango Petrified Forest (−3.894, −80.074) collected on 7 July 2011 by D. Salazar. Manabí: QCAZ 3604, subadult from Jipijapa (−1.357, −80.591, 259 m asl) collected on 27 December 1996 by G. Onore; QCAZ 947 from La Plata Island (−1.283, −81.066 15 m asl) collected on 12 August 1990 by A. Lansdale; QCAZ 13251, adult female from Manta river (−1.075, −80.736, 130 m asl) collected on 9 July 2014 by P. Picerno. Santa Elena: QCAZ 2158, adult female from Ancón (−2.317, −80.852, 36 m asl) collected on 19 October 1993 by V. Pérez; QCAZ 148, adult male from Santa Elena Península (−2.402, −80.679, 12 m asl) collected on 15 October 1994 by V. Pérez.

Etymology: The specific epithet *transandinus* is an adjective in the nominative singular and derives from the Latin words trans (=beyond) and andinus (=Andean). *Oxybelis transandinus* is the only South American species within the *Oxybelis aeneus* complex known to occur west of the Andes (i.e. trans-Andean).

Diagnosis: Among species of the *Oxybelis aeneus* complex (Jadin et al. 2020, 2021), *O. transandinus* can be distinguished from *O. acuminatus, O. aeneus*, and *O. inkaterra* (character states in parentheses) by having the second pair of chin shields in contact with each other for most of their length (mostly separated) and a distinct midventral stripe on first quarter of venter (absent). It further differs from *O. acuminatus* in having usually four infralabials (see Variation below) in contact with anterior chin shields (five) and second supralabial not in contact with preocular (in contact); from *O. aeneus* in having supraoculars longer than prefrontals (supraoculars equal in length or slightly longer than prefrontals), ventrals in females 176–187, mean = 182.2 ± 3.74 SD (184–203, mean = 192.1 ± 9.54 SD), subcaudals in females 147–168, mean = 160 ± 7.96 SD (146–184, mean = 168.2 ± 19.08 SD), ventrals in males 178–190, mean = 183 ± 5.09 (179–197,

mean = 188.8 ± 9.00 SD); from *O. inkaterra* in having supraoculars longer than prefrontals (equal in length), immaculate cream chin (heavily mottled), and in lacking eyespot markings on the posterior ventral surface of the body and tail (eyespot markings present). *O. transandinus* differs from *O. koehleri* in having a conspicuous midventral stripe (variable); last supralabial longer than first temporal (similar in length); immaculate cream chin in both sexes (medial red-brown stripe in females); ventrals 176–187 in females, mean = 182.2 ± 3.74 SD (184–191, mean = 187.57 ± 2.26 SD); subcaudals in females 147–168, mean = 160 ± 7.96 SD (176–189, mean = 184.8 ± 5.91 SD); from *O. microphthalmus* in having the preocular shorter than eye diameter (eye diameter shorter that preocular); ventrals 178–190 in males, mean = 183 ± 5.1 SD (184–202, mean = 192 ± 5.92 SD), 176–187 in females, mean = 182.2 ± 3.74 SD (184–204, mean = 193.58 ± 5.2 SD); subcaudals 147–168 in females, mean = 160 ± 7.96 SD (170–183, mean = 177.2 ± 4.22 SD); from *O. potosiensis* in having usually three supralabials in contact with orbit (two); conspicuous midventral stripe (variable); TL/SVL 0.59–0.66, mean = 0.62 ± 0.03 in females (0.7); ventrals 176–187 in females, mean = 182.2 ± 3.74 SD (186–195, mean = 191.67 ± 4.03 SD); from *O. rutherfordi* in having usually three supralabials in contact with orbit (two); usually nine supralabials (eight); posterior border of internasal extending beyond posterior border of supralabial I (posterior borders of both scales nearly aligned); subcaudals 147–168 in females, mean = 160 ± 7.96 SD (162–171, mean = 166.33 ± 3.25 SD); and from *O. vittatus* in having usually nine supralabials (eight); posterior border of internasal extending beyond posterior border of supralabial I (posterior borders of both scales nearly aligned); slightly constricted snout (tapered and terminally rounded); ventrals 176–187 in females, mean = 182.2 ± 3.74 SD (182–193, mean = 186.83 ± 4.02 SD); TL/SVL in males 0.65–0.73, mean = 0.67 ± 0.04 SD (0.73–0.76, mean = 0.74 ± 0.01 SD) and 0.59–0.66, mean = 0.62 ± 0.03 SD in females (0.62–0.84, mean = 0.74 ± 0.01 SD).

Description of holotype: QCAZ 17097, male, SVL = 63.9 cm, TL = 42.4 cm. Head distinct from neck, 3.4 times longer than broad and ~3.3 times longer than high; eye slightly protuberant, visible from anterior and lateral aspects, with circular pupil, eye diameter 15.3% head length; rostral 2.4 times wider than high; prefrontal fused with loreal, longer than broad, ~1.6 times the length of internasal, in contact with its mate medially, frontal, supraocular, and preocular posteriorly, nasal and internasal anteriorly, and supralabials II and III ventrally; frontal bell shaped, 2.4 times longer than wide, slightly longer than supraoculars, 0.81 times the length of eye-nostril distance, and shorter than the distance from its anterior edge to tip of snout; supraocular 2.3 times longer than wide, in contact with frontal medially, prefrontal anteriorly, preocular anterolaterally, eye laterally, upper postocular posterolaterally, and parietal posteriorly; parietals approximately hexagonal, in contact with four scales posteriorly; interparietal suture shorter than length of frontal and 1.6 times shorter than distance between frontal and tip of snout; nasal single, pierced by small nostril (~21.7% length of nasal scale), in contact with rostral anteriorly, internasal dorsally, prefrontal posteriorly and supralabials I and II ventrally; preocular one; postoculars two; temporal formula 1+2; nine supralabials on left side, dorsally in contact with nasal (I, II), prefrontal (II, III), preocular (III–V), eye (V, VI), lower postocular (VI), anterior temporal (VII–IX), and

Table 3. Selected meristic and morphometric characters for *Oxybelis transandinus*. Range (first line) and mean ± standard deviation (second line) are presented when appropriate.

Character	All specimens N = 18	Males N = 4	Females N = 10
Dorsal scale rows on neck	17	17	17
Dorsal scale rows at midbody	17	17	17
Dorsal scale rows anterior to cloaca	13 (94%) 14 (6%)	13	13 (90%) 14 (10%)
Ventrals	176–190 182.3 ± 3.69	178–190 183 ± 5.1	176–187 182.2 ± 3.74
Subcaudals	147–173 162.69 ± 7.32	161–173 168.8 ± 5.32	147–168 160 ± 7.96
Preoculars	1	1	1
Postoculars	2	2	2
Supralabials	7–10 8.69 ± 0.72	8–9 8.63 ± 0.52	7–10 8.58 ± 0.77
Supralabials entering orbit	5, 4–5, 5–6, 3–4–5, 4–5–6, 5–6–7 usually 4–5–6	5–6, 4–5–6 usually 4–5–6	5, 4–5, 5–6, 3–4–5, 4–5–6, 5–6–7 usually 4–5–6
Infralabials	7–10 9 ± 0.72	8–10 9 ± 0.64	7–10 9 ± 0.79
Temporal formula	1 + 1, 1 + 2, 2 + 2 usually 1 + 2	1 + 2	1 + 1, 1 + 2, 2 + 2 usually 1 + 2
Maximum SVL	–	73.1 cm	99.1 cm
Maximum total length	–	124.2 cm	157.8 cm
Tail length/SVL	–	0.65–0.73 0.67 ± 0.04	0.59–0.66 0.62 ± 0.03
Tail length/total length	–	0.39–0.42 0.40 ± 0.01	0.37–0.4 0.38 ± 0.01

posterior lower temporal (IX); eight supralabials on right side, dorsally in contact with nasal (I, II), prefrontal (II, III), preocular (III, IV), eye (IV–VI), lower postocular (VI, VII), anterior temporal (VII–VIII), and posterior lower temporal (VIII); infralabials 9/10 (left/right), first pair in contact medially posterior to mental, I–IV/I–V in contact with anterior genial, IV–VI/V–VII in contact with posterior genial; posterior genials in contact medially along ~55% of their total length, separated posteriorly by four smaller scales, of which the anterior two are tiny; dorsal scales smooth, in 17-17-13 rows; ventrals 181; anal plate divided; subcaudals 161, divided.

Colouration in life (Figure 2): Dorsal background pale brown, with a series of ~35 faint, dark transverse bands on anterior half of body formed by black pigment covering less than one-fourth of individual scales; dorsum of posterior half of body and tail speckled with black and dark brown; dorsal surface of head pale brown with dark pigment irregularly distributed and a dark line along medial edge of parietals; thin dark stripe on dorsal edge of supralabials and ventral edge of adjacent head scales extending from nasal scale to about six scales posterior to last supralabial; supralabials otherwise yellowish cream; short, light stripe from dorsal aspect of preocular, along lateral edge of supraocular and dorsal half of upper preocular to lateral aspect of parietal; infralabials and ventral surface of head immaculate cream; ventral surface of anterior quarter or body cream, with a pale brown midventral stripe that becomes gradually wider posteriorly; light medial line along brown midventral stripe; ventral surface of remaining body and tail pale brown with cream and dark brown freckles.

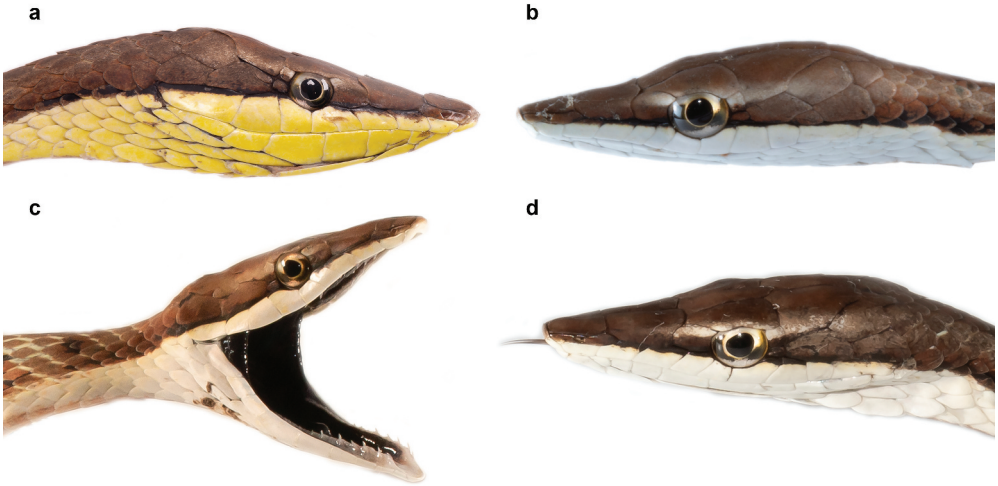

Figure 4. Heads of *Oxybelis transandinus* **sp. nov**. in lateral view. Paratypes QCAZ 15804 (A), 16039 (B), 17096 (C), and 14448 (D). Photographs by G. Pazmiño-Otamendi (A), D. Núñez (B, C), F. Ayala-Varela (D).

Variation: Variation in meristic and morphometric characters in *Oxybelis transandinus* is presented in Table 3. Most specimens have nine supralabials, with three (4–5–6) entering the orbit. Female specimen QCAZ 15804 has seven supralabials on right side, with 4–5 entering orbit, and eight on left side (3–4–5 entering orbit), whereas three specimens (QCAZ 8731, 16039, 16631) have 10 supralabials on at least one side, with 5–6–7 entering orbit (Figure 4). Female specimen QCAZ 3947 has eight supralabials on both sides, with only one (5) entering orbit on right side and two (4–5) on left side. Most specimens (16 out of 20) have four infralabials in contact with anterior chin shields on both sides; two specimens share the same condition on one side only, with three and five infralabials, respectively, in contact with anterior chin shields on the other side; one specimen has three and another five infralabials on both sides in contact with anterior chin shields. *Oxybelis transandinus* is a sexually dimorphic species, with females having fewer subcaudals and shorter tails than males (Table 3). Bogert and Oliver (1945) reported 22–27 maxillary teeth, 28–29 dentary teeth, 13 palatine teeth, and 13 pterygoid teeth in specimens of '*O. aeneus*' from Paramba (western Ecuador), which based on geographic distribution presumably correspond to *O. transandinus*.

Distribution and natural history: *Oxybelis transandinus* is known from the Pacific lowlands of Ecuador between sea level and 1,044 m in elevation (Figure 5). Most specimens were found in dry ecosystems including Deciduous Forest (annual mean temperature = 24.4 C, annual mean precipitation = 879.6 mm) and Dry Shrub (24.5 C, 548.3 mm); a few individuals were collected in Western Foothill Forest (22.3 C, 1,919.6 mm) (Ron 2020). Specimens were found active during the day, either on the

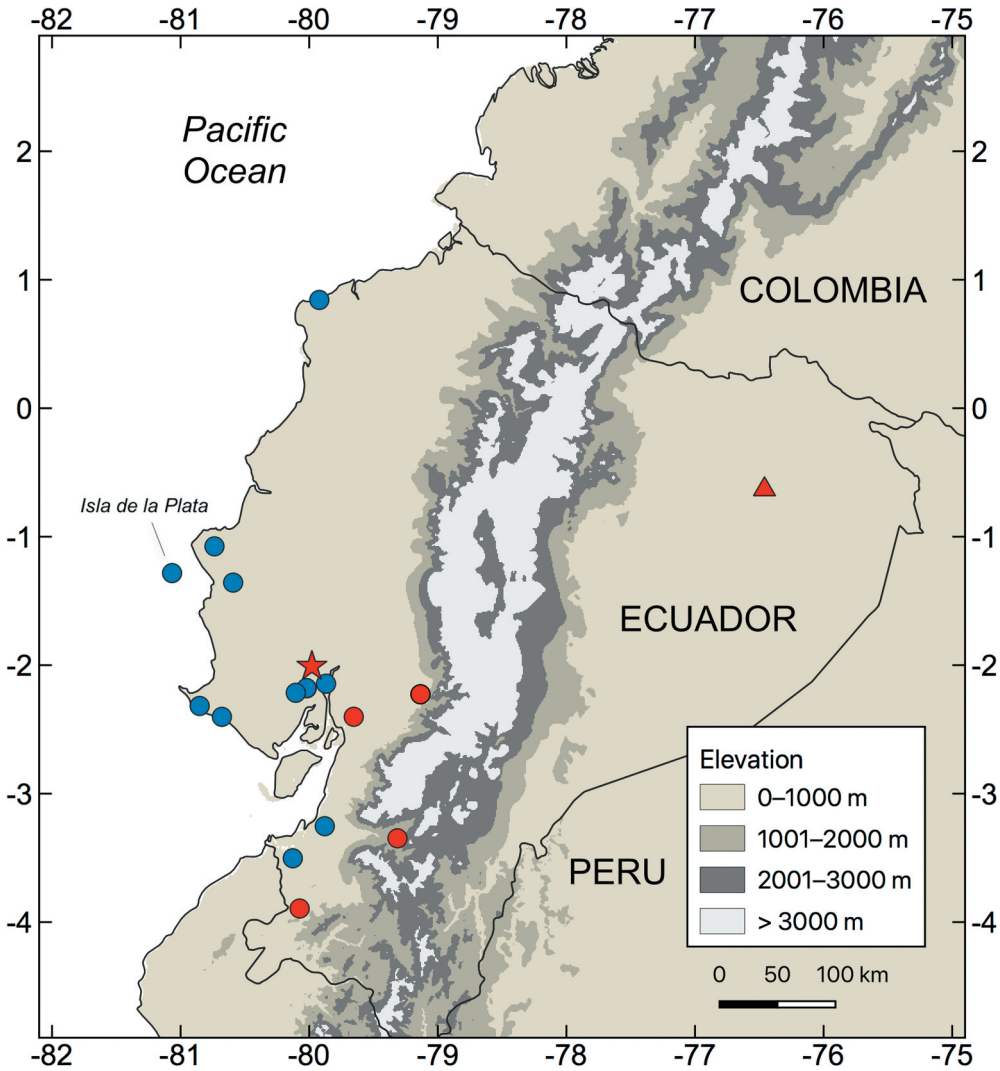

Figure 5. Known distribution of *Oxybelis transandinus* **sp. nov**. (circles) and *O. inkaterra* (triangle) in Ecuador. Star represents type locality of *O. transandinus*. Specimens sequenced in this study are shown in red.

ground or 1.5 m above it, or sleeping at night on leaves or branches up to 4 m above the ground. When disturbed, this species exhibits its dark purple mouth mucosa with a gaping mouth defensive behaviour (Figure 4).

Discussion

Our results are congruent with previous phylogenetic hypotheses (Jadin et al. 2019, 2020) in that Neotropical vine snakes are nested in three major clades, with green vine snakes (*O. fulgidus, O. wilsoni*) as sister to the clade (*O. brevirostris, O. aeneus* complex). Remarkably, the brown vine snake *O. aeneus* sensu lato was recently split into eight

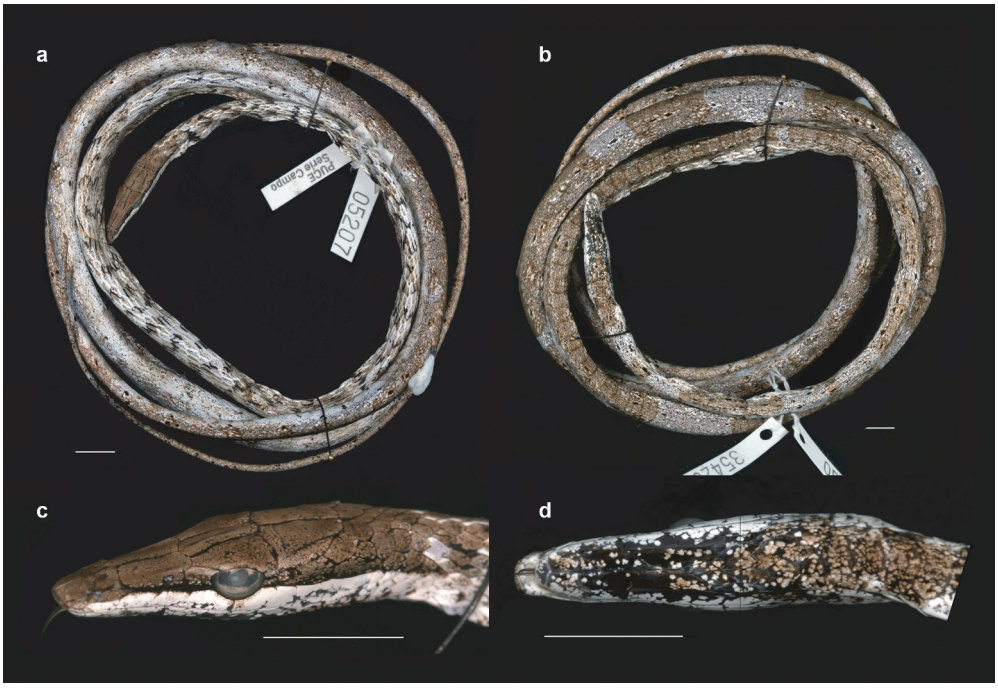

Figure 6. Specimen of *Oxybelis inkaterra* from Ecuador (QCAZ 5207) in dorsal (A) and ventral (B) views. Close-up of head in dorsal (C) and ventral (D) views. Photographs by J. Carrión. Scales bars = 10 mm.

species based on morphological and molecular evidence, as well as geographic distribution (Jadin et al. 2020, 2021), thereby revealing one of the best examples of cryptic diversity among Neotropical snakes. Notably, this recent work excluded the well-known populations of '*O. aeneus*' from west of the Andes in northern South America (Keiser 1974, 1982). In this paper, we analysed the first trans-Andean samples of the *O. aeneus* complex from Ecuador, which led to the discovery of a ninth species within this complex.

In agreement with previous studies, we recovered a paraphyletic *O. fulgidus*, with samples from Central America forming a clade sister to *O. wilsoni* (Figure 1). This species pair is sister to a strongly supported clade from South America, which includes samples from Suriname (S. Mackessy, pers. comm.), Venezuela, French Guiana, Ecuador, and Brazil (GenBank accession numbers MK209203 [12S], MK209278 [CYTB], and MK209316 [16S] correspond to specimen MZUSP11417 from Mato Grosso, Brazil; F. Grazziotin pers. comm.). Application of the name *O. fulgidus* to either the Central America or the South American clade is a complex problem because the holotype is lost and the original type locality is Santo Domingo, surroundings of Port-au-Prince, where this species does not occur. Strinkingly, Suriname, SE Peru and E Mexico have been proposed as type localities of *O. fulgidus* by different authors (Wallach et al. 2014). A taxonomic revision of *O. fulgidus* is underway as an attempt to clarify the taxonomic status of populations from Central and South America currently assigned to this species.

In this paper, we also provide new insights into the taxonomic identity of *O. aeneus* sensu stricto. Although Jadin et al. (2020) split this species into six species and restricted the name *O. aeneus* to populations from the Amazon Basin, they did not explicitly include samples of *O. aeneus* sensu stricto in their phylogenetic analyses. However, within their 'Northern South America' clade (see Figure 5 in Jadin et al. 2020), which they described as *O. rutherfordi*, the most basal sample (HM565765) was referred to as of unknown origin; but according to GenBank, this sample corresponds to voucher specimen R6911, which was collected in Luiz Eduardo Magalhães Hydroelectric Powerplant [−9.755 N, −48.373 W], municipality of Lageado, state of Tocantins (F. Grazziotin, pers. comm.), Brazil, approximately 1,925 km (airline) SE of the type locality of *O. aeneus* (Tefé, state of Amazonas, −3.350 N, −64.700 W). Therefore, here we assign temporarily specimen R6911 to *O. aeneus* sensu stricto based on distribution range (Jadin et al. 2020), but we recognise that only a thorough geographical sampling of *O. aeneus* across Amazonia will lead to a better taxonomic assessment. In general, we believe that recent taxonomic work on *O. aeneus* sensu lato has overlooked important morphological structures, such as cranial osteology and hemipenial morphology, which might be relevant for the systematics of this group. For example, Bogert and Oliver (1945) reported variation in skull morphology, with specimens from Mexico having more elongated prefrontal bones than specimens from Ecuador. Similarly, Keiser (1974) reported great variation in size and ornamentation of hemipenes. Therefore, a systematic revision of these morphological structures is needed to better assess species limits within the *O. aeneus* complex.

Unpublished samples from GenBank also revealed a putative undescribed species (*Oxybelis* sp.) from Escudo de Veraguas Island off the Caribbean coast of Panama. Surprisingly, the single specimen from this locality included in our analyses (USNM 347529) did not nest with specimens of *O. vittatus* from nearby localities in Panama. Instead, this specimen is nested in a strongly supported clade (BS = 87, PP = 1) along with *O. koehleri* (Guatemala to Costa Rica) and *O. potosiensis* (eastern Mexico and Belize) (Figure 1, S1). Although only 16S data was available for USNM 347529, we believe that incomplete gene sampling is not misplacing this specimen 'outside' *O. vittatus* because other samples of *O. vittatus* in our phylogeny are also represented by 16S only (CH 5078, 6080). Escudo de Veraguas Island (a.k.a. Isla Escudo) is the first of the islands of Bocas del Toro to separate from the mainland ~9,000 years ago by postglacial events (e.g. rising sea levels) and has been isolated ever since leading to marked morphological differentiation and even speciation of some mammals like bats and sloths (Anderson and Handley 2002). Therefore, although better sampling is desirable, it is reasonable to suggest that the specimen of *Oxybelis* from Isla Escudo belongs to an undescribed species.

Finally, we report the first record of *O. inkaterra* from Ecuador (Figure 6) based on a single specimen (QCAZ 5207) from Yasuni National Park in northern Amazonian Ecuador with diagnostic character states, such as upper labials three and four in contact with preocular, dorsum dirty cream with dark flecking, head heavily pigmented with black ventrally, and 'eyespot' markings on the ventral surface of the body and tail (Jadin et al. 2021). Furthermore, we include *O. inkaterra* for the first time in a phylogenetic analysis,

which revealed an Amazonian/northern-South-American clade (*O. inkaterra*, (*O. aeneus, O. rutherfordi*)). This clade supports the idea of a single invasion of South America from Central America within the *O. aeneus* complex (Jadin et al. 2019). However, the lack of resolution in the phylogenetic position of *O. transandinus*, which occurs in northwestern South America, creates uncertainty on the origin of South American species of the *O. aeneus* complex.

Acknowledgements

We are thankful to Stephen Mackessy and Felipe Grazziotin for providing locality data of specimens listed in GenBank. We also thank Daniel Mulcahy for sharing sequences of *Oxybelis* from Panama, as well as Robert Jadin and an anonymous reviewer for their great reviews of earlier versions of this manuscript. Specimens from Ecuador were collected under permits 005 RM-DPAM-MAE, 003-15 IC-FAU-DNB/MA, 003-17 IC-FAU-DNB/MA, 011-2018-IC-FAU-DNB/MA and Contrato Marco de Acceso a Recursos Genéticos MAE DNB-CM-2014-0002, MAE-DNB-CM-2015-0025 issued by Ministerio del Ambiente de Ecuador. Molecular work was supported by the Secretaría de Educación Superior, Ciencia, Tecnología e Innovación (SENESCYT) under the 'Arca de Noé' Initiative (Santiago Ron and OTC principal investigators) and PUCE-DGA (OTC principal investigator).

Disclosure statement

No potential conflict of interest was reported by the author(s).

Funding

This work was supported by the Pontificia Universidad Católica del Ecuador; Secretaría de Educación Superior, Ciencia, Tecnología e Innovación [Arca de Noé].

ORCID

Omar Torres-Carvajal http://orcid.org/0000-0003-0041-9250

References

Anderson RP, Handley CO Jr. 2002. Dwarfism in insular sloths: biogeography, selection, and evolutionary rate. Evolution. 56:1045–1058. doi:10.1111/j.0014-3820.2002.tb01415.x.

Arévalo ES, Davis SK, Sites JW Jr. 1994. Mitochondrial DNA sequence divergence and phylogenetic relationships among eight chromosome races of the *Sceloporus grammicus* complex (Phrynosomatidae) in central Mexico. Syst Biol. 43:387–418. doi:10.1093/sysbio/43.3.387.

Bogert CM, Oliver JA. 1945. A preliminary analysis of the herpetofauna of Sonora. Bull Am Mus Nat Hist. 83:297–426.

Burbrink FT, Lawson R, Slowinski JB. 2000. Mitochondrial DNA phylogeography of the polytypic North American rat snake (*Elaphe obsoleta*): a critique of the subspecies concept. Evolution. 54:2107–2118. doi:10.1554/0014-3820(2000)054[2107:MDPOTP]2.0.CO;2.

Deng W, Maust BS, Nickle DC, Learn GH, Liu Y, Heath L, Mullins JI, Mullins JI. 2010. DIVEIN: a web server to analyze phylogenies, sequence divergence, diversity, and informative sites. BioTechniques. 48:405–408. doi:10.2144/000113370.

Dowling HG. 1951. A proposed standard system of counting ventrals in snakes. B J Herpetol. 1:97–99. doi:10.2307/1437542.

Guindon S, Dufayard J-F, Lefort V, Anisimova M, Hordijk W, Gascuel O. 2010. New algorithms and methods to estimate maximum-likelihood phylogenies: assessing the performance of PhyML 3.0. Syst Biol. 59:307–321. doi:10.1093/sysbio/syq010.

Jadin RC, Blair C, Jowers MJ, Carmona A, Murphy JC. 2019. Hiding in the lianas of the tree of life: molecular phylogenetics and species delimitation reveal considerable cryptic diversity of New World Vine Snakes. Mol Phylogenet Evol. 134:61–65. doi:10.1016/j.ympev.2019.01.022.

Jadin RC, Blair C, Orlofske SA, Jowers MJ, Rivas GA, Vitt LJ, Murphy JC, Smith EN, Murphy JC. 2020. Not withering on the evolutionary vine: systematic revision of the Brown Vine Snake (Reptilia: Squamata: *Oxybelis*) from its northern distribution. Org Divers Evol. 20:723–746. doi:10.1007/s13127-020-00461-0.

Jadin RC, Jowers MJ, Orlofske SA, Duellman WE, Blair C, Murphy JC. 2021. A new vine snake (Reptilia, Colubridae, *Oxybelis*) from Peru and redescription of *O. acuminatus*. Evol Syst. 5:1–12. doi:10.3897/evolsyst.5.60626.

Katoh K, Standley DM. 2013. MAFFT multiple sequence alignment software version 7: improvements in performance and usability. Mol Biol Evol. 30:772–780. doi:10.1093/molbev/mst010.

Kearse M, Moir R, Wilson A, Stones-Havas S, Cheung M, Sturrock S, Drummond A, Cooper A, Markowitz S, Duran C. 2012. Geneious Basic: an integrated and extendable desktop software platform for the organization and analysis of sequence data. Bioinformatics. 28:1647–1649. doi:10.1093/bioinformatics/bts199.

Keiser ED Jr. 1974. A systematic study of the neotropical vine snake *Oxybelis aeneus* (Wagler). Bull Texas Memorial Mus. 22:1–51.

Keiser ED Jr. 1982. *Oxybelis aeneus*. Catalogue Ame Amphibians Reptiles. 305:305.1–305.4.

Knight A, Mindell DP. 1994. On the phylogenetic relationship of Colubrinae, Elapidae, and Viperidae and the evolution of front-fanged venom systems In snakes. Copeia. 1994(1):1–9. doi:10.2307/1446664.

Kocher TD, Thomas WK, Meyer A, Edwards SV, Pääbo S, Villablanca FX, Wilson AC. 1989. Dynamics of mitochondrial DNA evolution in animals: amplification and sequencing with conserved primers. Proc Natl Acad Sci USA. 86:6196–6200. doi:10.1073/pnas.86.16.6196.

Lanfear R, Calcott B, Ho SYW, Guindon S. 2012. Partition-Finder: combined selection of partitioning schemes and substitution models for phylogenetic analyses. Mol Biol Evol. 29:1695–1701. doi:10.1093/molbev/mss020.

Lanfear R, Frandsen PB, Wright AM, Senfeld T, Calcott B. 2017. PartitionFinder 2: new methods for selecting partitioned models of evolution for molecular and morphological phylogenetic analyses. Mol Biol Evol. 34:772–773. doi:10.1093/molbev/msw260.

Lawson R, Slowinski JB, Crother BI, Burbrink FT. 2005. Phylogeny of the Colubroidea (Serpentes): new evidence from mitochondrial and nuclear genes. Mol Phylogenet Evol. 37:581–601. doi:10.1016/j.ympev.2005.07.016.

Melo-Sampaio PR, Passos P, Prudente ALC, Venegas PJ, Torres-Carvajal O. 2021. Systematic review of the polychromatic ground snakes *Atractus snethlageae* complex reveals four new species from threatened environments. J Zool Syst Evol Res. 59:718–747. doi:10.1111/jzs.12453.

Miller M, Pfeiffer W, Schwartz T. 2010. Creating the CIPRES Science Gateway for 1100 inference of large phylogenetic trees. http://www.phylo.org/index.php/portal/cite_us .

Palumbi SR, Martin A, Romano S, McMillan WO, Stice L, Grabowski G. 1992. The simple fool's guide to PCR, version 2.0. Honolulu: University of Hawaii.

Peters JA. 1960. The Snakes of Ecuador: a checklist and key. Bull Mus Comp Zool. 122:491–541.

Rambaut A. 2018. FigTree version 1.4 (Version 1.4.4.). http://tree.bio.ed.ac.uk/software/figtree .

Rambaut A, Drummond AJ. 2019a. LogCombiner version 1.10.5. http://beast.bio.ed.ac.uk .

Rambaut A, Drummond AJ. 2019b. TreeAnnotator version 1.10.5. http://beast.bio.ed.ac.uk .

Roll U, Feldman A, Novosolov M, Allison A, Bauer AM, Bernard R, Meiri S, Castro-Herrera F, Chirio L, Collen B. 2017. The global distribution of tetrapods reveals a need for targeted reptile conservation. Nat Ecol Evol. 1:1677–1682. doi:10.1038/s41559-017-0332-2.

Ron SR. 2020. Regiones naturales del Ecuador. BIOWEB. Pontificia Universidad Católica del Ecuador. https://bioweb.bio/faunaweb/reptiliaweb/RegionesNaturales .

Ronquist F, Teslenko M, van der Mark P, Ayres DL, Darling A, Höhna S, Larget B, Liu L, Suchard MA, Huelsenbeck JP. 2012. MrBayes 3.2: efficient Bayesian phylogenetic inference and model choice across a large model space. Syst Biol. 61(3):539–542. doi:10.1093/sysbio/sys029.

Stamatakis A. 2014. RAxML Version 8: a tool for phylogenetic analysis and post-analysis of large phylogenies. Bioinformatics. 30:1312–1313. doi:10.1093/bioinformatics/btu033.

Stamatakis A, Hoover P, Rougemont J. 2008. A rapid bootstrap algorithm for the RAxML Web servers. Syst Biol. 57:758–771. doi:10.1080/10635150802429642.

Torres-Carvajal O, Hinojosa KC. 2020. Hidden diversity in two widespread snake species (Serpentes: Xenodontini: *Erythrolamprus*) from South America. Mol Phylogenet Evol. 146:106772. doi:10.1016/j.ympev.2020.106772.

Townsend TM, Alegre RE, Kelley ST, Wiens JJ, Reeder TW. 2008. Rapid development of multiple nuclear loci for phylogenetic analysis using genomic resources: an example from squamate reptiles. Mol Phylogenet Evol. 47:129–142. doi:10.1016/j.ympev.2008.01.008.

Wallach V, Williams KL, Boundy J. 2014. Snakes of the world. A catalogue of living and extinct species. Boca Raton (FL): CRC Press.